# Unitary interaction geometries in few-body systems

Lorenzo Contessi,[1,2] Johannes Kirscher,[3,4,5] and Manuel Pavon Valderrama[6]

[1] *Université Paris-Saclay, CNRS-IN2P3, IJCLab, 91405 Orsay, France*
[2] *IRFU, CEA, Université Paris-Saclay, 91191 Gif-sur-Yvette, France*
[3] *Department of Physics, SRM University–AP, Amaravati 522502, Andhra Pradesh, India*
[4] *Theoretical Physics Division, School of Physics and Astronomy, The University of Manchester, Manchester M13 9PL, United Kingdom*
[5] *Institute for Nuclear Studies, Department of Physics, The George Washington University, Washington, D.C. 20052, USA*
[6] *School of Physics, Beihang University, Beijing 100191, China*

(Received 9 March 2023; revised 9 January 2024; accepted 5 February 2024; published 19 March 2024)

We consider few-body systems in which only a certain subset of the particle-particle interactions is resonant. We characterize each subset by a *unitary graph* in which the vertices represent distinguishable particles and the edges resonant two-body interactions. Few-body systems whose unitary graph is connected will collapse unless a repulsive three-body interaction is included. We find two categories of graphs, distinguished by the kind of three-body repulsion necessary to stabilize the associated system. Each category is characterized by whether the graph contains a loop or not: for tree-like graphs (graphs containing a loop) the three-body force renormalizing them is the same as in the three-body system with two (three) resonant interactions. We show numerically that this conjecture is correct for the four-body case as well as for a few five-body configurations. We explain this result in the four-body sector qualitatively by imposing Bethe-Peierls boundary conditions on the pertinent Faddeev-Yakubovsky decomposition of the wave function.

DOI: 10.1103/PhysRevA.109.032217

## I. INTRODUCTION

Systems in which the two-body scattering length is considerably larger than the range of the interaction are called unitary or resonant. They show properties that are independent of the details of their interparticle interaction (provided it has a finite range) [1], which is why it is referred to as *universality*. The reason is the presence of an exceedingly large separation of scales: the ratio between the scattering length and any other lengthscale of the system basically tends to infinity. As a consequence, unitary two-body systems can be described by a parameter-free (or universal) theory.

The consequences of universality beyond the two-body case are more interesting and counterintuitive. Three-boson systems for which the two-boson interaction is resonant exhibit a characteristic geometric spectrum in which the ratio of the binding energies of the $n$th and $(n+1)$th excited states is constant and universal. This spectrum (usually referred to as the Efimov effect) was predicted in the 1970s [2] and confirmed experimentally a decade and a half ago [3]. Similar geometric spectra have been predicted for larger boson clusters [4], systems of nonidentical particles [5–7], mass-imbalanced $P$- and even $D$-wave three-body states [8], and so on. From the point of view of symmetry, what is happening here is that the continuous scale invariance of universal two-body systems becomes anomalous and breaks in the three-body case as a consequence of the quantization process, yet it survives as discrete scale invariance. The unitary three-body system is thus no longer parameter-free. It acquires a three-body parameter that can be identified with the binding energy of the fundamental three-body bound state.

This raises the question of what happens with systems of four or more particles in the unitary limit. We know [9] that the four-body parameter is not needed to predict the ground state of the four-bosons system and it only appears as a perturbative correction together with finite-range corrections. However, this is not necessarily the case for all four-body systems if not all particles interact resonantly. For four-body systems of the $AABB$ type, with $A$ and $B$ denoting two different species of particles (either bosons or distinguishable) and where only the $AB$ interaction is resonant, the three-body parameters that are required to define the $AAB$ and $ABB$ subsystems are insufficient to determine the binding energy of the ground state [10]. Expressed differently, the $AABB$ system is a rare example in which a four-body parameter is required.

Conversely, not all universal few-body systems acquire a three-body parameter. The $P$-wave three-body system with equal mass particles (or, equivalently, the $AAB$ system if $A$ are fermions and $m_A = m_B$) does not collapse or exhibit the Efimov effect. For specific mass imbalances, this system forms three-body bound states whose binding energies depend only on the two-body scattering length [11] and only when the mass imbalance is large enough will it require a three-body parameter and display a geometric spectrum. Another example is the $AABB$ system when the two species are fermions, in which case there will be no bound state [12].

Going back to the nonfermionic case (here we consider distinguishable particles), the present paper generalizes the methods and findings of Ref. [10] as follows: instead of considering different types of two-species clusters, we will focus on the geometry of their resonant interactions. In particular, we will characterize few-body systems in terms of a *unitary graph*, here defined as a graph whose vertices and lines represent, respectively, the particles and resonant interactions of the system. Provided the graph is connected, the few-body system

 ©2024 American Physical Society

requires the definition of a three-body parameter. If the graph is a tree, the required three-body parameter will be that of the three-body system with two unitary pairs (e.g., the *AAB* or *ABB* systems we discussed in the previous paragraph). If the graph contains a cycle (a loop), the three-body parameter of the unitary three-boson system will be needed instead. We tested the previous two statements explicitly in the four- and five-body systems.

Furthermore, we expect that all the few-body system represented by connected graphs will display the Efimov effect. We conjecture that the geometric ratios between the binding energies of the $n$th and $(n+1)$th bound state will be $(1986.1)^2$ and $(22.7)^2$ for tree-like graphs and graphs containing cycles, respectively. These ratios represent the ones that are found in the three-body systems when there are two and three unitary pairs [13]. The key assumption for this conjecture is that all systems with the same Efimov ratios are renormalized by the same three-body force. We provide a heuristic argument explaining the scaling behavior to be expected in certain $N > 3$ systems as well as the type of three-body force required to renormalize the corresponding unitary graphs.

## II. THEORY AND METHODOLOGY

### A. Description of the $N$-body system

We consider nonrelativistic $N$-body systems described by the Schrödinger equation

$$\left(-\frac{\hbar^2}{2m}\sum_{i}^{N}\vec{\partial}_i^2+\hat{v}\right)\Psi_N=E_N\,\Psi_N, \tag{1}$$

where $\Psi_N=\Psi_N(\vec{r}_1,\dots,\vec{r}_N)$ is the wave function, $\vec{\partial}_i=\frac{d}{d\vec{r}_i}$ is the derivative with respect to the coordinate of particle $i$, $\hat{v}$ is the potential, and $E_N$ is the center-of-mass energy of the $N$-body system. We limit the discussion to distinguishable, equal-mass $m$ particles, and hence no permutation symmetry is enforced on the wave function $\psi_{1,\dots,N}$. We note that it is, in principle, possible to extend the previous description to systems with a mass imbalance, though we will not consider this case in the present paper.

For a general $N$-body system, the interaction potential $\hat{v}$ may include up to $N$-body forces. The unitary systems investigated here demand two- and three-body forces, only. That is, we have

$$\hat{v}=\sum_{i<j}v_{ij}+\sum_{i<j<k}w_{ijk}, \tag{2}$$

with $v_{ij}$ and $w_{ijk}$ the two- and three-body potentials

Unitary two-body systems are insensitive to the range of their interaction, which is never probed. As a consequence, the two-body potential is effectively reduced to a contact-range potential, i.e., a Dirac delta in r-space. This type of potential is singular and has to be regularized, e.g., by including a cutoff in the calculations. For concreteness we choose a Gaussian regulator in coordinate space

$$v_{ij}=v(\boldsymbol{r}_i,\boldsymbol{r}_j)=c_{ij}(\lambda)\,e^{-\lambda^2\frac{(r_i-r_j)^2}{4}}, \tag{3}$$

where $\lambda$ is the cutoff (i.e., the auxiliary range we introduce to make numerical calculations easier) and $c_{ij}$ a coupling constant. This coupling depends on the cutoff [that is, $c_{ij}=c_{ij}(\lambda)$] in such a way as to keep the two-body system at unitarity for arbitrary values of the cutoff $\lambda$, provided the interaction of the particle pair $ij$ is unitary in the first place. The coupling and cutoff dependence is identical for every unitary two-body subsystem, and thus we write

$$c_{ij}(\lambda)=c(\lambda)\,f_{ij}, \tag{4}$$

with $f_{ij}=0$ or 1 for nonunitary and unitary $ij$, respectively. The cutoff dependence of regularized contact interactions is well known [14] and becomes $c(\lambda)\propto\lambda^2$ in our specific case (i.e., in our normalization of the regularized Dirac delta, see Eq. (13) for a more detailed explanation).

Due to the breaking of scale invariance, the three-body systems are sensitive to the range of the interaction even after the two-body system is properly renormalized. To be explicit, while the two-body system is invariant with respect to $\vec{r}\to\kappa\vec{r}$ transformations for arbitrary $\kappa$, in the three-body system this symmetry only survives for $\kappa=\kappa_0$ with $\kappa_0$ being a specific real number (e.g., the $\kappa_0\approx 22.7$ scaling factor for the Efimov effect in the three-boson system [2]). In practical terms, this manifests as a cutoff dependence of the ground state of the three-body system, whose binding energy will diverge as $\lambda^2$.

The inclusion of a three-body force stabilizes the energy of the three-body ground state and removes the unphysical cutoff dependence [15,16]. With a Gaussian regulator the three-body force reads

$$w_{ijk}=w(\boldsymbol{r}_i,\boldsymbol{r}_j,\boldsymbol{r}_k)=d_{ijk}(\lambda)\sum_{cyc}e^{-\lambda^2\left[\frac{(r_i-r_j)^2}{4}+\frac{(r_i-r_k)^2}{4}\right]}, \tag{5}$$

where *cyc* are the cyclical permutations of $ijk$, and $d_{ijk}(\lambda)$ and its running are determined by the condition of reproducing the ground state (or an arbitrary excited state) of the $ijk$ three-body system (this requires that at least two pairs of particles within the $ijk$ set are unitary). If we assume that the ground-state energy of every bound three-body subsystem is the same, we can make the additional simplification

$$d_{ijk}(\lambda)=d(\lambda)\,g_{ijk}, \tag{6}$$

with $g_{ijk}=0$ or 1 depending on the particular $ijk$ three-body subsystem under consideration (we will specify this in the following lines).

### B. Characterization of the few-body configurations as unitary graphs

We are interested in few-body systems where not all of the $N$ particles interact resonantly, but only a subset of them. The rest of the pairs (i.e., the nonunitary ones) are considered to be noninteracting: in principle, their interaction can be treated as a perturbative correction around the unitary limit set by the unitary pairs. The reason is that the scattering lengths of the nonunitary pairs are arbitrarily smaller than the scattering lengths of the unitary pairs. However, owing to the breakdown of continuous-scale invariance for $N\geqslant 3$, for the previous expansion to be valid there is the additional proviso that the ratio between the three-body scale (e.g., the characteristic lengthscale or size of the three-body bound state) and any scale associated with the residual nonresonant interactions

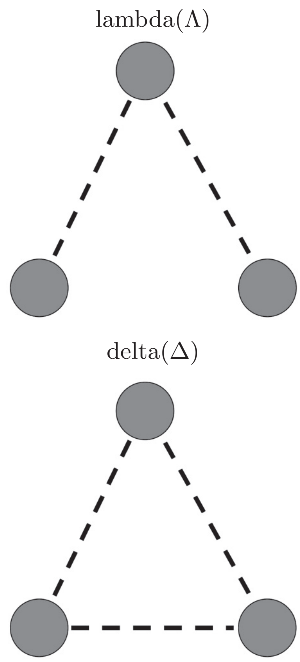


FIG. 1. Three-body systems with two (Λ) and three (Δ) resonant pairs: the gray circles and dashed lines represent the distinguishable particles and their unitary interactions, respectively.

(e.g., the scattering length of the nonunitary pairs of particles) should be large.

Here, we describe (partially) unitary $N$-body systems in terms of *unitary graphs*, a graph in which vertices correspond to particles and lines to unitary interactions. The sets of three- and four-body configurations we consider and their names are shown in Figs. 1 and 5. These are all the possible connected graphs with three and four vertices. For the graphs with three vertices (Fig. 1) we denote them as follows:

(3a) *delta* or Δ (for its resemblance to the Greek letter), which is also the fully connected graph with three nodes and

(3b) *lambda* or Λ (again, relating to the Greek letter).

For four-vertex graphs (Fig. 5) we introduce the following:

(4a) the *full* (the fully connected graph with four nodes);

(4b) the *circle-slash*[1] or simply *slash* (which is also referred to as the *diamond* in the literature [17]);

(4c) the *circle*;

(4d) the *line* (self-explanatory);

(4f) the *paw*, as it is often referred to (other names are the *3-pan* graph or the *(3,1)-tadpole* graph[2]); and

(4g) the *star*, which we previously named *dandelion* in Ref. [10], and also referred to as the *claw* [17].

[1]Of all shown graphs, this is the only one not amenable to a straightforward $N$-vertex generalization.

[2]A $k$-pan is a graph with $(k+1)$ points, where $k$ of the points are connected in such a way that they form a cycle and with the odd point connected to one of the points within that $k$-cycle (see Fig. 1.2 in Ref. [17]); a $(k, m)$ tadpole is a $k$ cycle where one of the points within the cycle is connected to a tail of $m$ connected points (i.e.,, an $m$ line).

A few of the previous graphs are easily generalizable to the $N$-body case. However, if not stated otherwise, we will be referring to the four-body version of the graph. In some cases, we might indicate the $N$-body generalizations by adding the number of points in the graph to its name, e.g., the 5-full, the 6-circle, the 7-line, or the 8-star graphs.

The $N$-body potential $\hat{v}$ associated with these systems or graphs is fully determined by the set of $ij$ pairs and $ijk$ triplets for which the two- and three-body interaction is nonzero, i.e., the $ij$ and $ijk$ for which the $f_{ij}$ and $g_{ijk}$ factors defined in Eqs. (4) and (6) are equal to 1, $f_{ij}=1$ and $g_{ijk}=1$. For the two-body forces this is trivial: $f_{ij}=1$ if the pair $ij$ are connected by a line when we look at the corresponding unitary graph (and $f_{ij}=0$ if the pair is not connected).

For the three-body forces, the characterization of the $ijk$ triplets for which $g_{ijk}=1$ is relatively simple for the Δ and Λ three body systems: $g_{123}=1$. However, it becomes more involved in the four-body case, at least, in principle (in practice, concrete calculations accept a very convenient simplification that we will comment later). The explicit definition of the $g_{ijk}$ coefficients depends on whether or not a particular graph contains a Δ subgraph:

(i) if it contains a Δ subgraph, $g_{ijk}=1$ if and only if $f_{ij}=1$, $f_{jk}=1$ and $f_{ik}=1$, i.e., if the particle pairs $ij$, $jk$, and $ik$ are all unitary

(ii) while if there is no Δ subgraph, it will be only necessary that two of the $ij$, $jk$, and $ik$ pairs are unitary.

That is, there is a three-body force for each Δ triplet, or if there is none, for each Λ triplet. Alternatively, we might define the two following sets of relevant two- and three-body interactions for the previous graphs

$$\mathcal{F}_{\rm graph} = \{(i,j): i,j \in \{1,\dots,N\},\ i<j, f_{ij}\neq 0\}, \tag{7}$$

$$\mathcal{G}_{\rm graph} = \{(i,j,k): i,j,k \in \{1,\dots,N\},\ i<j<k,\ g_{ijk}\neq 0\}, \tag{8}$$

With $\mathcal{F}_{\rm graph}$ and $\mathcal{G}_{\rm graph}$ it is possible to redefine the potential as

$$\hat{v} = \sum_{(i,j)\in\mathcal{F}_{\rm graph}} v_{ij} + \sum_{(i,j,k)\in\mathcal{G}_{\rm graph}} w_{ijk}, \tag{9}$$

where the definitions of $v_{ij}$ and $w_{ijk}$ do not involve dependence on the indices for the couplings

$$v_{ij} = c(\lambda)\, e^{-\lambda^2 \frac{(r_i-r_j)^2}{4}}, \tag{10}$$

$$w_{ijk} = d(\lambda) \sum_{cyc} e^{-\lambda^2\left[\frac{(r_i-r_j)^2}{4}+\frac{(r_i-r_k)^2}{4}\right]}, \tag{11}$$

that is, with the definition of $\mathcal{F}_{\rm graph}$ and $\mathcal{G}_{\rm graph}$ we can now dispense of the $f_{ij}$ and $g_{ijk}$ factors previously found in Eqs. (4) and (6).

However, numerically we observe that the inclusion of the three-body force on all the triplets, even the not strictly necessary ones to avoid collapse, does not affect the predictions for the four-body ground-state energies. We can explain this by the fact that contact range three-body forces have little impact on noncollapsing triplets of particles.

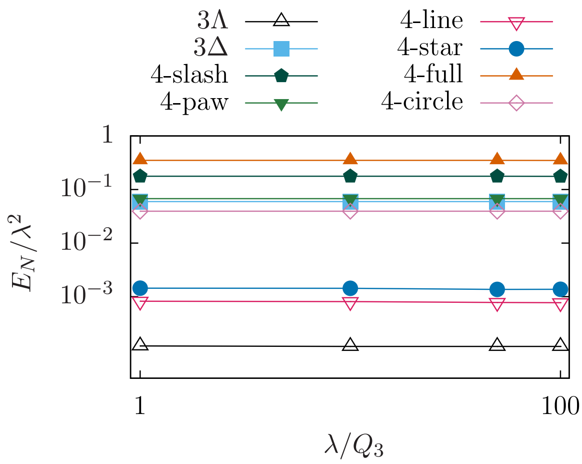


FIG. 2. Regulator dependence of the three- and four-body ground-state binding energies without any collapse-preventing three-body interaction. The lines highlight the $\propto \lambda^2$ dependence of the binding energies of the states.

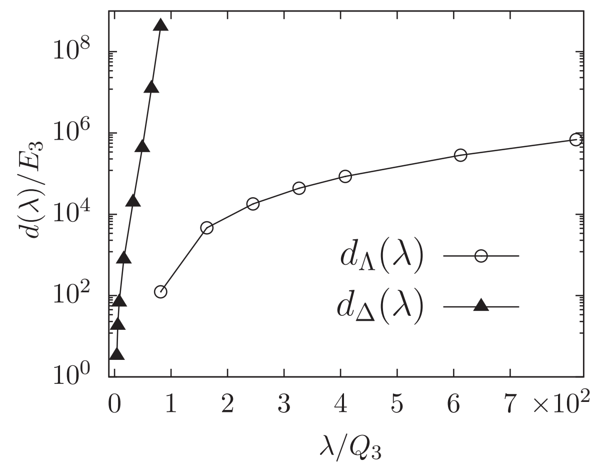


FIG. 3. The running of the three-body coupling strength $d(\lambda)$ which renormalizes the fully resonant (filled triangles) and the two-pair resonant (empty circles) three-body systems to a single bound state.

### C. Practical implementation

For all calculations in this work, we set $\hbar = c = 1$, and the particle mass to unity: $m = 1$. All the momenta, included the parameter $\lambda$ are defined by the typical three-body momentum

$$Q_3 = \sqrt{\frac{3}{2} m|E_3|}, \tag{12}$$

and all energies can be related with the energy of the three-body system $E_3$. The coupling strength $c(\lambda)$ is chosen to induce an $S$-wave scattering length of $a_0 = 10^6\, Q_3$. We calibrated the three-body coupling $d(\lambda)$ as to generate a three-body ground state with binding energy $E_3$. This numerical value for $E_3$ was chosen identical for both three-body configurations of Fig. 1, that is, for the $\Lambda$ (two resonant pairs) and $\Delta$ (three resonant pairs) configurations.

All conclusions in this work are drawn from the dependence of the ground-state solution of Eq. (1) on the cutoff $\lambda$ and on the unitary graph representing the $N$-body system. We calibrate $c(\lambda)$ by solving the two-body Schrödinger equation at zero energy with a standard Numerov integration algorithm. For the three-body coupling $d(\lambda)$ and for the calculations of the ground-state energies $E_N$ for $N \geqslant 3$, we use two different variational methods, both of which optimize a set of Gaussian basis functions: the stochastic-variational method (SVM) [18] and the refined-resonating-group method (RGM) [19]. All $N \geqslant 3$ calculations employed the SVM, and we used the RGM as an additional verification of the values of $E_N$ in the three- and four-body systems for a subset of cutoffs.

### D. Cutoff dependence of the couplings

With the parameters and methods specified, we obtain the expected, above-mentioned cutoff dependence for the two-body strength: $c(\lambda) \propto \lambda^2$. In our notation, the $c$ absorbs factors stemming from the Gaussian regularization of the Dirac delta, i.e.,

$$v_{ij} = C(\lambda)\, \delta_\lambda(\vec{r}_i - \vec{r}_j) = C(\lambda)\, \frac{\lambda^3\, e^{-\lambda^2 \frac{(\vec{r}_i - \vec{r}_j)^2}{4}}}{8\pi^{3/2}}, \tag{13}$$

from which the relation between $c(\lambda)$ and the more commonly used $C(\lambda)$

$$c(\lambda) = \frac{\lambda^3}{8\pi^{3/2}}\, C(\lambda), \tag{14}$$

is obtained. If we take into account that $C(\lambda) = -\frac{2\pi^2}{m\lambda}\theta^{-1}$ [20], with $\theta$ a regulator-dependent number, it is apparent that we should indeed have $c(\lambda) \propto \lambda^2$.

If we use the two-body potential with the coupling of Eq. (14) and in the absence of a three-body force, the calculated three-body ground-state energy diverges as the square of the cutoff, i.e., $E_3 \propto \lambda^2$. This is explicitly shown in Fig. 2 for the two configurations of Fig. 1 (the $\Delta$ and $\Lambda$ configurations) where a parabolic fit to these numerical results finds that

$$\frac{E_{3\Delta}}{E_{3\Lambda}} \simeq 505.1. \tag{15}$$

That is, we find a more rapid collapse of the fully resonant $\Delta$ configuration compared with the $\Lambda$ configuration.

These three-body collapses are avoided by including the three-body contact terms in Eq. (5). The coupling $d(\lambda)$ is calibrated under the condition that the energy of the three-body ground state remains constant with the cutoff. Numerically, we determine $d_\Delta(\lambda)$ by stabilizing $E_{3\Delta}$ and $d_\Lambda(\lambda)$ fixing $E_{3\Lambda}$. The corresponding values can be found in Fig. 3.[3]

Even though we limit ourselves to the calculation of the ground state of the $\Delta$ and $\Lambda$ trimers, the excited states of these

[3]Our choice for the cutoff interval, $\lambda < 1.22\, Q_3$ for $d_\Delta(\lambda)$ and $\lambda < 12.25\, Q_3$ for $d_\Lambda(\lambda)$, follows numerical constraints. The collapse of the unrenormalized system is expressed in separately diverging ground-state expectation values of the kinetic energy and two-body potential operators. The latter does so more rapidly with $\lambda$, and hence, the diverging binding energy is itself a result of the cancellation of two even larger numbers. The repulsion required thus from a three-body counterterm demands strengths that approach numerical limits faster for the fully resonant system (see Fig. 3).

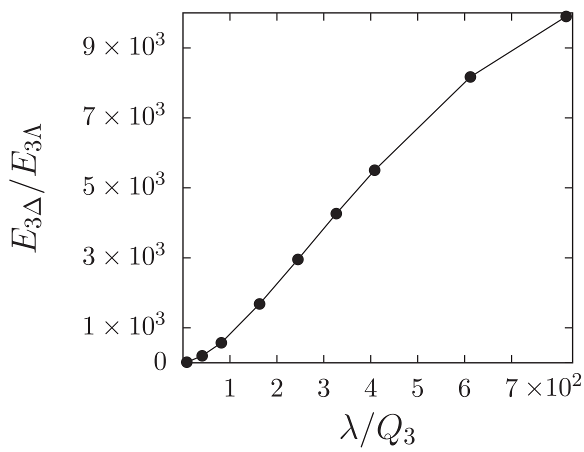


FIG. 4. Divergent behavior of ground-state energy $E_{3\Delta}$ of the $\Delta$ three-body system (three resonant pairs) when we include the three-body force that renormalized the $\Lambda$ three-body system (two resonant pairs).

systems do in principle display the Efimov effect [2]. We did not check the two geometric factors that characterize the Efimov spectra specifically in this work. Yet the $\Delta$ configuration collapses more rapidly than the $\Lambda$, which reflects the smaller scaling factor of the first (22.7 for the $\Delta$) compared to the second (1986.1 for the $\Lambda$). We demonstrate this by employing the $d_\Lambda$ to the $\Delta$ which yields the divergence plotted in Fig. 4.

## III. FOUR-BODY SECTOR

### A. Renormalization

Next, we consider all unitary four-body systems in which the resonant two-body interactions form a connected graph. There are six such configurations which we list in Fig. 5.

In the absence of three-body forces, the ground-state energy of each of these four-body configurations exhibits the quadratic collapse with respect to the regulator $\lambda$ that we encountered in the three-body case, Eq. (15). The reason is the presence of at least one $\Delta$ or $\Lambda$ subgraph in each of the connected four-body graphs. These subgraphs will collapse in the absence of three-body forces as discussed in the previous section.

The inclusion of a three-body force (see Sec. II) solves the problematic collapse. However, there is an ambiguity regarding which three-body force to use: as shown in the previous section, the three-body coupling $d(\lambda)$ defined in Eq. (5) has two possible solutions depending on whether the three-body systems is $\Delta$- or $\Lambda$-shaped. In our calculations, only one choice for the running of $d$ with $\lambda$ was able to properly renormalize the system and generate a finite binding energy. Our numerical results for employing the two runnings in the various graphs (Fig. 5) are summarized graphically in Fig. 6. From these results, we infer the following correspondence between a unitary graph and the running of the three-body force:

(i) the full, slash, paw and circle graphs require $d_\Delta(\lambda)$;
(ii) the line and the star graphs require $d_\Lambda(\lambda)$.

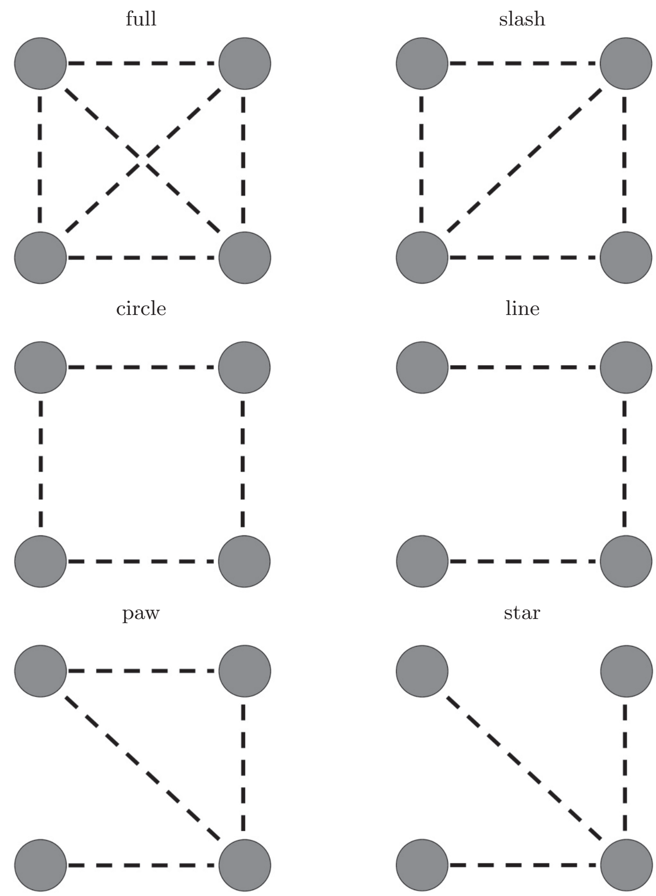


FIG. 5. Configurations of four distinguishable particles (gray vertices) for which their resonant pair interactions (dashed lines) form a connected graph.

This is a rather intuitive result, except for the circle: we would expect that the renormalization of a four-body system will only require a $\Delta$-type three-body coupling $d_\Delta(\lambda)$ if its unitary graph contains one or more $\Delta$-shaped subgraphs. Conversely, if there are only $\Lambda$-type subgraphs, a $d_\Lambda(\lambda)$ coupling should suffice. This is indeed what happens in five of the six configurations where, as we will see, this behavior can be understood in terms of a relatively simple heuristic argument grounded on the Bethe-Peierls boundary conditions for each of these systems. The circle is a remarkable exception: numerically we find that it requires $d_\Delta(\lambda)$ (the three-body coupling that renormalizes the $\Delta$-shaped three-body system) although it does not contain $\Delta$ subgraphs.

In the upper panel of Fig. 6 we show the cutoff dependence of the four-body binding energy for the configurations that require $d_\Delta(\lambda)$. The quantitative ratios we find are

$$E_{4\text{-full}} = 4.4(1)\, E_{3\Delta}, \tag{16}$$

$$E_{4\text{-slash}} = 1.8(1)\, E_{3\Delta}, \tag{17}$$

$$E_{4\text{-paw}} \approx 1.0\, E_{3\Delta}, \tag{18}$$

$$E_{4\text{-circle}} \approx 0.2\, E_{3\Delta}, \tag{19}$$

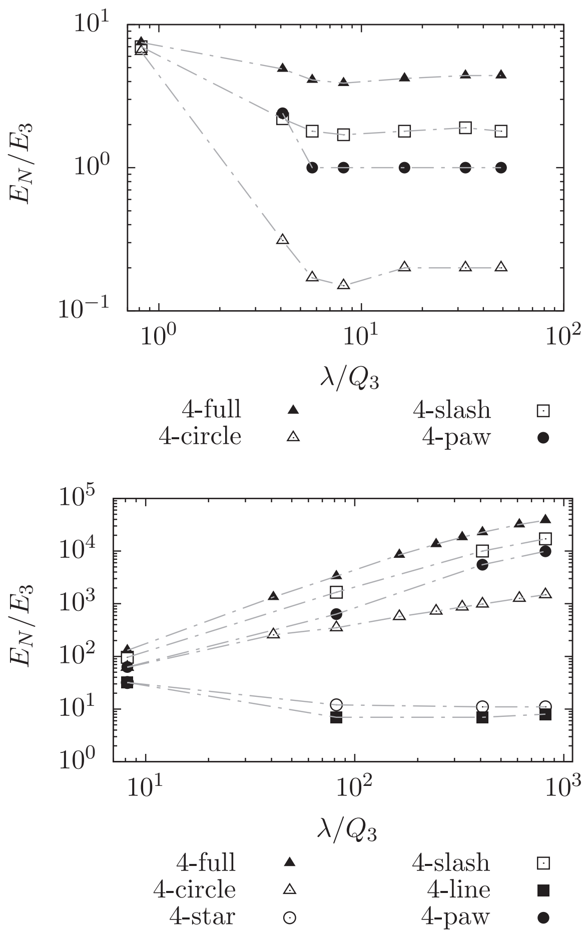


FIG. 6. Regulator dependence of the ground-state energy of the six four-body configurations if the running of the three-body counterterm is set in the fully resonant three-body system (upper panel, $d_\Delta$) and in the two-pair-resonant three-body system (lower panel, $d_\Lambda$).

where for the full configuration we reproduce the well-known relation between the binding energy of the unitary three- and four-boson system. For the circle, the four-body binding energy is smaller than the three-body $\Delta$-type configuration. This is not a problem because the circle cannot decay into a three-body $\Delta$ bound system and a free particle. Notice that the line and star configurations (including the three-body $\Lambda$ system) are not shown in the upper panel of Fig. 6 simply because when $d_\Delta(\lambda)$ is applied to them it happens to be too repulsive to allow for a bound state below the three-body threshold.

Now, if we use the $d_\Lambda(\lambda)$ coupling instead, only the line and star configurations converge, while the full, slash, paw, and circle collapse (see lower panel of Fig. 6). For the line and star configurations, we find

$$E_{4\text{-star}} = 11(1)\, E_{3\Lambda}, \tag{20}$$

$$E_{4\text{-line}} = 8(1)\, E_{3\Lambda}. \tag{21}$$

These ratios are not of order one. They are also certainly larger than the respective ratios for the full, slash, paw, and circle.

### B. Combinatorial approximation to binding

The renormalized binding energy ratios that we calculated reveal an intriguing pattern: they are proportional to the number of interacting triplets in that system. First, we consider the $\Delta$-like configurations (except the 4-circle, which is the four-body system that behaves in a more peculiar way). The number of interacting triplets is

$$4 : 2 : 1, \tag{22}$$

for the full, slash, and paw configurations, respectively. This is to be compared with the ratios of their binding energies

$$4.4(1) : 1.8(1) : 1. \tag{23}$$

For the $\Lambda$-like configurations (star and line) the number of interacting triplets is

$$3 : 2, \tag{24}$$

while the ratios of their binding energies are

$$2.8(6) : 2, \tag{25}$$

and thus in agreement with the ratios of interacting triplets. The uncertainties result from propagating the errors in the binding energies of the different configurations. The previous ratios differ up to a certain extent from the naive approximation of counting the number of three-body subgraphs, which is to be expected owing to the simplicity of the argument. Yet, the concrete reasons that might explain these discrepancies in a more quantitative manner remain an open question.

Another prediction that can be derived from the combinatorial argument is noteworthy: the binding energy of the $N$-body full configuration. For this prediction, we have to first consider the paw configuration, i.e., a $\Delta$ graph with a fourth particle interacting resonantly with one of the particles forming the $\Delta$. Owing to the resonant nature of this interaction, the expectation is that the binding energy of the odd particle with the $\Delta$ three-body subsystem will be just below the $\Delta$ plus free particle threshold, which is precisely what is expressed by Eq. (18). In fact, this argument could be extended for an $N$-body system composed of a $\Delta$ followed by a line of $N-3$ particles (the $N$-paw or the $(3, N-3)$-tadpole graph) for which the binding energy will approximately be that of the three-body $\Delta$ system:

$$E_{N\text{-paw}} \approx 1.0\, E_{3\Delta}. \tag{26}$$

Thus, the $N$-paw is stabilized very close to the decay threshold into a $\Delta$ and a $(N-3)$ particle. This approximation assumes that the three-body repulsion required to stabilize the $N$-paw system is the same as the one of the $\Delta$-system. This particular repulsion implies that the binding energy of the subsystem formed by the line of $N-3$ particles approaches zero. We corroborated Eq. (26) with numerical calculations for $N=4$ for multiple cutoffs and $N=5$ for a single cutoff $\lambda \sim 100\, Q_3$ [see Eqs. (18) and (32)].

If we return now to the full $N$-body system, the previous assumption together with the combinatorial hypothesis leads to the following ansatz:

$$E_{N\text{-full}} \approx \binom{N}{3} E_{3\Delta} \approx \frac{N(N-1)(N-2)}{6} E_{3\Delta} \approx \{1, 4, 10, 20, 35, 56 \dots\} E_{3\Delta} \quad \text{for } N = 3, 4, 5, 6, 7, 8 \dots, \tag{27}$$

where in the second line we specified the values for different numbers of particles. This approximation eventually breaks as $N$ increases. For contact-range forces, in general, we expect that for high-enough $N$ the binding energy of these systems will display *saturation*, that is, a binding energy proportional to the number of particles $N$. As the ground state of the *full* $N$-body system is as bound as the unitary $N$-boson system,[4] we can compare our results with the ratios obtained for the latter, which have been extensively studied in the literature. If we use the ratios obtained in Ref. [21]

$$E_{N\text{-full}} = \{1.0, 4.7, 10.6, 18.6, 27.9, 38.9 \dots\} E_{3\Delta} \quad \text{for } N = 3, 4, 5, 6, 7, 8 \dots, \tag{28}$$

then we see that even though the combinatorial argument works well for $N \leqslant 6$ eventually its uncertainties end up increasing with $N$ (about $18, 6, 7, 21, 31\%$ for $N = 4, 5, 6, 7, 8$). If we use instead the more recent calculation of the authors of Ref. [22], the ratios for $N = 3, 4, 5$ will be in better agreement with our approximation

$$E_{N\text{-full}} = \{1.0, 4.2, 9.5, 16.3 \dots\} E_{3\Delta} \quad \text{for } N = 3, 4, 5, 6 \dots, \tag{29}$$

though we are limited to $N \leqslant 6$ in this case. Finally, as the number of particles grows, saturation properties emerge (i.e., $E_{N\text{-full}}$ becomes proportional to $N$, as has been shown in Ref. [4]) and our combinatorial approximation will cease to be valid.

## IV. 5-CIRCLE AND THE UNITARY LOOP CONJECTURE

Next, we consider five-body unitary systems. In this case there are a large number of connected unitary graphs (21 configurations[5]) and for practical reasons we will focus on a few unitary geometries only. For the same reasons, our current investigation is limited to less than six bodies.

The specific five-body configurations we study are the 5-full, 5-circle, 5-star, 5-line, and 5-paw graphs as shown in Fig. 7. The reasons for this selection are the following:

(i) to verify that the 5-full or 5-paw and 5-star or 5-line configurations are renormalized by the $d_\Delta(\lambda)$ and $d_\Lambda(\lambda)$ couplings, respectively, and

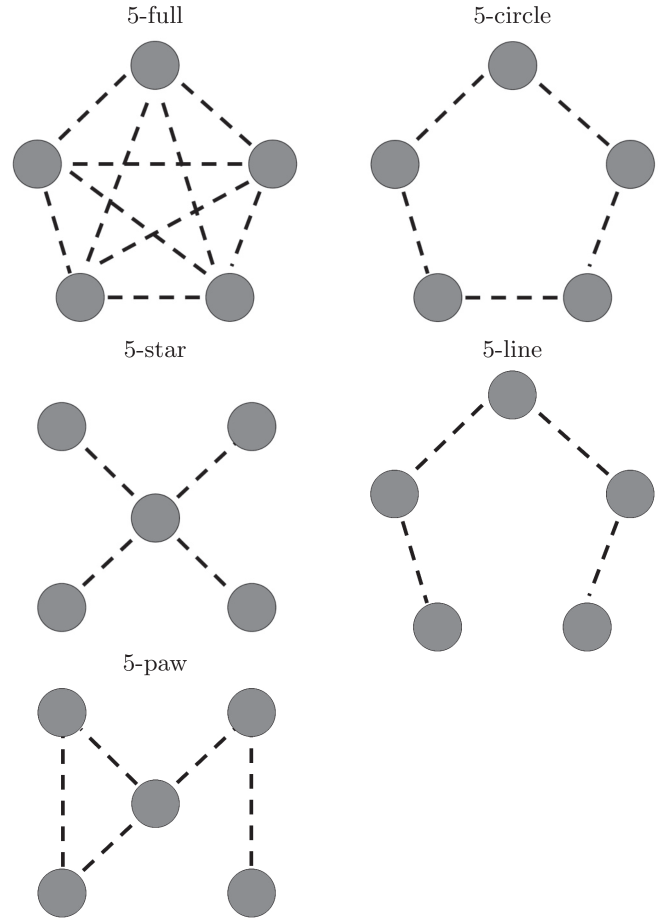


FIG. 7. The three connected five-body shapes considered in this work.

(ii) to further confirm the exceptional status of the circle in the five-body case, i.e., the fact that its proper renormalization requires the $d_\Delta(\lambda)$ coupling despite not containing any $\Delta$ subgraph;

(iii) to test the conjecture that the binding energy of the $N$-paw approximately coincides with that of the $\Delta$, Eq. (26) up to $N = 5$.

The three hypotheses do indeed hold: in the case of the 5-full and 5-circle configurations we numerically find[6] the binding energies to be

$$E_{5\text{-full}} \approx 10.8\, E_{3\Delta}, \tag{30}$$

$$E_{5\text{-circle}} \approx 0.06\, E_{3\Delta}. \tag{31}$$

We note, again, that the 5-circle cannot decay into other bound states. Hence, there is no problem with its binding energy being smaller than the three-body $\Delta$ system. For the 5-paw we find that

$$E_{5\text{-paw}} \approx 1.0\, E_{3\Delta}, \tag{32}$$

which confirms the validity of the approximation of Eq. (26) for the $N = 5$ case, with the caveat that we are actually unable

[4]The reason is the permutation symmetry of the full $N$-body system, which effectively implies that the $N$ particles behave as identical particles. Even though this allows both symmetric and antisymmetric configurations (bosonic and fermionic behaviors), the ground state will correspond to a fully symmetric configuration.

[5]The number of connected graphs for $N = 2, 3, 4, 5, 6, 7, 8, \dots$ is $1, 2, 6, 21, 112, 853, 11117, \dots$ (integer sequence A001349 in Ref. [23]; see Ref. [24] for an explicit calculation of their number up to $N = 18$).

[6]Results in this section were obtained for a subset of cutoff values between $10\, Q_3$ and $100\, Q_3$.

to distinguish within the accuracy of our calculations whether this is a genuine five-body state or a $3+1+1$ state. For the 5-star and the 5-line we have instead

$$E_{\text{5-star}} \approx 30\, E_{3\Lambda}, \tag{33}$$

$$E_{\text{5-line}} \approx 16\, E_{3\Lambda}, \tag{34}$$

which follows the trend of binding energies much larger than one, cf., the 4-star and 4-line, Eqs. (20) and (21). It is interesting to notice that the ratio of their energies is

$$1.9 : 1. \tag{35}$$

This complies with the conjecture that the ground-state energy scales as the number of interacting triplets in the system, which is

$$2 : 1, \tag{36}$$

corresponding to 6 and 3 triplets in the 5-star and the 5-line, respectively.

Both findings, those regarding the 4- and 5-circle, suggest the following conjecture: few-body systems whose unitary interactions form a graph containing a closed loop will be renormalized by the three-body force that renormalizes the three-body $\Delta$-shaped system (which, incidentally, can also be labeled as the 3-circle). Intuitively, this observations should hold for unitary systems containing 3-, 4-, or 5-circle subgraphs: if the circle component is not renormalized properly, neither will be the system of which it is a part. However, even though the general idea does not seem implausible, we have not found a rigorous proof yet.

Finally, a paradoxical situation is noteworthy. The $N$-circle and $N$-lines are locally identical as $N \to \infty$, i.e., if we only consider a finite number of particles, there is no difference between the $N \to \infty$ circle and line. Yet, we observe the binding energy of the circle to decrease with $N$ while that of the line increases. Unfortunately, without explicitly considering the thermodynamic limit, which requires a series of techniques completely different to those used in our paper, it is probable that the answer to this problem will remain elusive for the time being.

## V. EXPLAINING THE TWO FOUR-BODY RENORMALIZATION PATTERNS

The renormalization of the four-body unitary systems falls into two distinct patterns: $\Delta$- and $\Lambda$-like. Here we present a heuristic argument of why this is the case. We stress that this is not a rigorous derivation of those renormalization patterns, and yet, the explanation we provide, though incomplete, helps to clarify in which cases we should expect each type of three-body force.

For understanding the patterns we will consider a zero-range two-body resonant interaction. That is, we will be considering the $\lambda \to \infty$ (or zero-range) limit, in which a two-body resonant interaction is reduced to a boundary condition of the wave function at the origin, that is,

$$\frac{d}{dr_{lk}}[r_{lk}\Psi_N]\Big|_{r_{lk}=0} = 0, \tag{37}$$

for each $l, k$ particle pair for which the interaction is resonant ($\vec{r}_l$ and $\vec{r}_k$ are single-particle coordinates and $\vec{r}_{lk} = \vec{r}_l - \vec{r}_k$). The Faddeev-component expansion of the $N$-body wave function

$$\Psi_N = \sum_{ij} \psi_{ij}(\vec{r}_{ij}, \dots), \tag{38}$$

yields

$$\frac{d}{dr_{lk}}[r_{lk}\psi_{lk}] + \sum_{ij\neq lk} \psi_{ij}(\vec{r}_{ij}, \dots)\Big|_{r_{lk}=0} = 0. \tag{39}$$

In general, this set of equations will simplify owing to symmetries that reduce the number of independent Faddeev components. For instance, in the $N$-boson system or in the full $N$-body unitary system, all the Faddeev components will be identical, i.e., $\psi_{ij} = \psi$; in the first case this happens because of Bose-Einstein symmetry and in the second because of symmetry under the permutation group.

In the case of the three-body system, it is well known how to derive the Efimov scaling from the boundary condition in Eq. (37). We do not present here the full derivation for the three-body case, which can be found in Ref. [25]. Instead, we will try to understand the general patterns connecting the discrete scaling of three- and four-body systems. We will use the 3- and 4-full systems as a template and then discuss how results in these two configurations extend to the other cases. For the 3-full (i.e., $\Delta$) system, we find that the boundary condition for $lk = 12$ reads

$$\frac{d}{dr_{12}}[r_{12}\psi(\vec{r}_{12}, \vec{\rho}_3)]\Big|_{r_{12}=0} + \psi(\vec{r}_{23}, \vec{\rho}_1)\Big|_{r_{12}=0} + \psi(\vec{r}_{31}, \vec{\rho}_2)\Big|_{r_{12}=0} = 0. \tag{40}$$

Here we already took into account that the three Faddeev components of the wave function are formally identical, and $\vec{\rho}_k = \vec{r}_k - (\vec{r}_i + \vec{r}_j)/2$ (plus the condition $i \neq j \neq k$) being one of the Jacobi coordinates. After suitable manipulations, the previous boundary condition leads to the standard Efimov effect with a discrete scaling of 22.7 (the specific steps leading to this result are well-known, see, e.g., Ref. [13]).

If we now consider the 4-full system, we have in principle 6 identical Faddeev components corresponding to the 6 possible interacting pairs. The Faddeev components can be further subdivided into Faddeev-Yakubovsky components as follows:

$$\psi(\vec{r}_{12}, \dots) = \psi_K(\vec{r}_{12}, \vec{\rho}_3, \vec{\sigma}_4) + \psi_K(\vec{r}_{12}, \vec{\rho}_4, \vec{\sigma}_3) + \psi_H(\vec{r}_{12}, \vec{h}_{12-34}, \vec{r}_{34}), \tag{41}$$

plus the decompositions for all the permutations of particles 1, 2, 3, and 4, where we use the customary subscripts $K$ and $H$ to indicate the $K$- and $H$-components. For the $K$ set of Jacobi coordinates, we have $\vec{\rho}_{k(ij)} = \vec{r}_k - (\vec{r}_i + \vec{r}_j)/2$ (though usually the $ij$ subscript will be dropped, as it always corresponds to that of the first coordinate $\vec{r}_{ij}$) and $\vec{\sigma}_l = \vec{r}_l - (\vec{r}_i + \vec{r}_j + \vec{r}_k)/3$ with $i \neq j \neq k \neq l$, while for the $H$ set we only have one new coordinate: $\vec{h}_{ij-kl} = (\vec{r}_i + \vec{r}_j)/2 - (\vec{r}_l + \vec{r}_l)/2$.

Now we write down the boundary condition for the $lk = 12$ pair in terms of the Faddeev-Yakubovsky components and

Jacobi coordinates defined above:

$$\begin{aligned}
&\underbrace{\frac{d}{dr_{12}}[r_{12}\psi_K(\vec{r}_{12},\vec{\rho}_3,\vec{\sigma}_4)]\big|_{r_{12}=0}+\psi_K(\vec{r}_{23},\vec{\rho}_1,\vec{\sigma}_4)\big|_{r_{12}=0}+\psi_K(\vec{r}_{31},\vec{\rho}_2,\vec{\sigma}_4)\big|_{r_{12}=0}}_{A}\\
&+\underbrace{\frac{d}{dr_{12}}[r_{12}\psi_K(\vec{r}_{12},\vec{\rho}_4,\vec{\sigma}_3)]\big|_{r_{12}=0}+\psi_K(\vec{r}_{24},\vec{\rho}_1,\vec{\sigma}_3)\big|_{r_{12}=0}+\psi_K(\vec{r}_{41},\vec{\rho}_2,\vec{\sigma}_3)\big|_{r_{12}=0}}_{B}\\
&+\frac{d}{dr_{12}}\left[r_{12}\,\psi_H(\vec{r}_{12},\vec{h}_{12-34},\vec{r}_{34})+r_{12}\,\psi_H(\vec{r}_{34},\vec{h}_{34-12},\vec{r}_{12})\right]\big|_{r_{12}=0}\\
&+[\psi_H(\vec{r}_{23},\vec{h}_{23-14},\vec{r}_{14})+\psi_H(\vec{r}_{24},\vec{h}_{24-13},\vec{r}_{24})+\psi_H(\vec{r}_{14},\vec{h}_{23-14},\vec{r}_{23})+\psi_H(\vec{r}_{13},\vec{h}_{24-13},\vec{r}_{24})]\big|_{r_{12}=0}\\
&\underbrace{+[\psi_K(\vec{r}_{13},\vec{\rho}_4,\vec{\sigma}_2)+\psi_K(\vec{r}_{14},\vec{\rho}_2,\vec{\sigma}_2)+\psi_K(\vec{r}_{23},\vec{\rho}_4,\vec{\sigma}_1)+\psi_K(\vec{r}_{24},\vec{\rho}_3,\vec{\sigma}_1)+\psi_K(\vec{r}_{34},\vec{\rho}_2,\vec{\sigma}_1)+\psi_K(\vec{r}_{34},\vec{\rho}_1,\vec{\sigma}_2)]\big|_{r_{12}=0}}_{C}=0.
\end{aligned} \tag{42}$$

The boundary condition is the sum of three terms ($A$, $B$ and $C$ as defined by the underbraces) such that $A+B+C=0$. We note that $C$ encompasses the last 3 lines of the equation.

Contrary to what happens in the three-body system, it is far from evident how to solve the four-body boundary condition or what are the characteristics of its solution (e.g., its Efimov scaling). Yet, it happens that we have a good understanding of the spectrum of the unitary four-boson system: basically, for each Efimov trimer there are two tetramers with known binding energies [21,26–28]. This suggests on the one hand that the Efimov scaling of the three- and four-boson systems is identical and on the other that the tetramers can be understood as a fourth particle binding to an already existing trimer.

These numerical observations can be readily explained if we impose the assumption that $A=B=C=0$ simultaneously (instead of the less stringent $A+B+C=0$ condition). This can be explained as follows.

(i) The conditions $A=0$ and $B=0$ are just Eq. (40), except for the extra Jacobi coordinate at the end. Provided this coordinate can be factored out, it will be irrelevant for solving these two equations. As a consequence, if the previous assumption about factorization is correct, the $K$-components of the 4-full system will have the same Efimov scaling as the $\Delta$ three-body system.

(ii) The condition $C=0$ implies that the $H$-component is tied to the $K$-components and their Efimov scalings will be the same. The reason is that $C=0$ can be understood as an equation with two terms, one involving the $H$ components and a second involving the $K$ components:

$$C_H[\psi_H]+C_K[\psi_K]=0, \tag{43}$$

where $C_H$ and $C_K$ represent the parts containing $\psi_H$ and $\psi_K$ of the last 3 lines of Eq. (42). Here $\psi_K$ plays the role of an external term obtained from the conditions $A=0$ and $B=0$, while $\psi_H$ is derived from $\psi_K$. Thus, the resulting $H$-component will follow the scaling of the $K$-component. For the 4-full system we conjecture the existence of two different solutions for this $H$-component, explaining the observed pattern of two tetramers tied to every Efimov trimer. Yet, we notice that the present argument does not rule out the possibility of independent solutions of $C_H[\psi_H]=0$, which would result in the existence of tetramers that do not follow the discrete scaling of the $\Delta$ subsystem: if anything, these tetramers might only be discarded on the basis that they do not appear in numerical calculations.

That is, provided the previous assumptions are correct (we warn though that they do not necessarily apply to all unitary configurations, as we will review in the next few paragraphs), the conclusion will be that the 4-full system is renormalized by the same three-body force as in the $\Delta$ system.

Indeed the previous two assumptions are pretty strong and we suspect that they are not generally applicable to all unitary geometries. Instead, they are to be taken as a tentative explanation of the spectrum of the 4-full (or four-boson) system as already calculated numerically in Refs. [21,26–28]. Yet, we warn that other solutions might exist: for instance, we notice that if there were to be solutions of $A+B+C=0$ that do not comply with the $A=0$, $B=0$ and $C=0$ hypothesis, this will likely result in a second type of tetramers that do not follow the same scaling laws as the $\Delta$ system. If these additional solutions were to exist in the 4-full configuration, it might explain the controversy about the four-body parameter in the four-boson system [29–31].

The same arguments can be applied *mutatis mutandis* to all the other four-body configurations considered in this work, though the manipulations required can be quite involved. Provided that the $A=0$, $B=0$ and $C=0$ hypothesis is valid, the general conclusion is that a unitary graph will follow the smallest scaling of its subgraphs: if the graph contains a $\Delta$ subgraph the scaling factor will be 22.7, and if not it will be 1986.1. We observe that in general this seems to be correct (though this has only been checked for the ground state).

The exception to this rule is the 4-circle, which brings us back to the problem of the general validity of the two assumptions that we previously made. This configuration, despite not including $\Delta$ subgraphs, is not renormalized by the $\Lambda$ three-body force. Instead, the renormalization of the 4-circle seems to be achieved by using the $\Delta$ three-body force, as shown by our calculations. This implies that the $A=0$, $B=0$ and $C=0$ hypothesis is not valid for this configuration, where the most probable reason for its failure is that $C=0$ has by itself zero solutions. In turn, this means that the $A=0$ and $B=0$ conditions do not apply to the 4-circle (whose only solutions are probably those of the $A + B + C = 0$ condition). This explains why it does not follow the Efimov scaling of systems containing $\Lambda$ subgraphs.

Previous investigations about the 4-circle are not conclusive either. In Ref. [32] the 4-circle was conjectured to be renormalized by the three-body force of the $\Lambda$ system (and thus have a discrete scaling of 1986.1). Yet, the ground-state energy of the 4-circle was found to be unnaturally large, $\sim 400\ E_3$, which might indicate that the system is, in fact, collapsing. More recently, the authors of Ref. [31] found that the geometric scaling of the four-body two-species system with a mass imbalance is smaller than the corresponding scaling of its three-body counterpart, which is consistent with our assumption about the scaling of the 4-circle ($22.7 < 1986.1$). However, the arguments in Ref. [31] depend explicitly on the existence of a large difference in masses between the two species and are thus not directly applicable to our 4-circle configuration. Even though there are no clear-cut contradictions in the previous two studies, we consider that more attention to the spectral structure of the 4-circle will be needed to determine its discrete scaling properties.

## VI. CONCLUSIONS

We analyzed partially unitary few-body systems in which all particles have the same mass but not all interparticle interactions are resonant, only a subset of them. Each of these few-body systems can be characterized by a unitary graph whose vertices and lines represent particles and resonant interactions, respectively. The resonant interactions can be modeled, without loss of generality, by zero-range potentials, which are singular and require regularization and renormalization. Here, we analyzed the renormalization of the ground states of systems with $N = 3$ and 4 particles (plus a few illustrative $N = 5$ configurations).

From a series of numerical calculations and qualitative arguments, we conjecture a relation between the geometry of the unitary graph representing the partially unitary system and its renormalization. Partially unitary few-body systems do display Thomas collapse, i.e., the binding energies of these systems diverge as the range of their interactions approach zero. As in the three-body case, this collapse is avoided by the inclusion of a zero-range, repulsive three-body force which stabilizes the binding energy of the ground state. The type of three-body force renormalizing a partially unitary four-body system (of which there are six, see Fig. 5) depends on the properties of the unitary graph of the latter:

(i) unitary tree-like graphs require the three-body force that renormalizes the three-body system with two resonant pairs (which we have called the $\Lambda$ system);

(ii) unitary graphs containing closed loops are renormalized instead by the three-body force of the three-body system with three resonant pairs (which we called the $\Delta$ system).

We deduced (and verified) this renormalization pattern numerically for each of the four-body unitary graphs. We conjecture that this pattern extends to partially unitary systems with $N > 4$, though we have only verified this generalization numerically for three selected $N = 5$ systems.

Furthermore, we proposed a heuristic argument that exploits the representation of a resonant pair in terms of a Bethe-Peierls boundary condition to show that the different four-body unitary graphs are indeed expected to be renormalized by the three-body force of the $\Lambda$- or $\Delta$-shaped systems. More specifically, what we showed is that the resonant two-body interaction imposes a constraint on the four-body wave function that is identical to the analogous constraint for the three-body system (modulo the presence of an additional coordinate for the extra particle). Incidentally, this is the same constraint that generates the characteristic discrete scale invariance of 22.7 and 1986.1 for the $\Delta$- and $\Lambda$-shaped three-body systems. Hence, we conjecture that the discrete scaling properties of a particular unitary graph will follow one of these two patterns (depending on whether they are renormalized by the three-body force of the $\Delta$- or $\Lambda$-shaped systems). However, the argument fails for the particular case of cyclic graphs (the $N$-circles in the naming convention we follow) which indicates that our explanation of this behavior is incomplete, representing an intriguing open problem which is left to future work.

## ACKNOWLEDGMENTS

We owe thanks to H. W. Grießhammer and N. Barnea for insightful discussions and critical comments. J.K. was supported by the STFC ST/P004423/1, the U.S. Department of Energy under Contract No. DE-SC0015393, and the hospitality of The George Washington University and The Hebrew University. M.P.V. is partly supported by the National Natural Science Foundation of China under Grants No. 11735003, No. 11835015, No. 11975041, No. 12047503, and No. 12125507, the Fundamental Research Funds for the Central Universities and the Thousand Talents Plan for Young Professionals. M.P.V. would also like to thank the IJCLab of Orsay, where part of this work was done, for its long-term hospitality.

[1] E. Braaten and H.-W. Hammer, Phys. Rep. **428**, 259 (2006).
[2] V. Efimov, Phys. Lett. B **33**, 563 (1970).
[3] T. Kraemer, M. Mark, P. Waldburger, J. G. Danzl, C. Chin, B. Engeser, A. D. Lange, K. Pilch, A. Jaakkola, H.-C. Nägerl, and R. Grimm, Nature (London) **440**, 315 (2006).
[4] J. Carlson, S. Gandolfi, U. van Kolck, and S. A. Vitiello, Phys. Rev. Lett. **119**, 223002 (2017).
[5] K. Helfrich, H.-W. Hammer, and D. S. Petrov, Phys. Rev. A **81**, 042715 (2010).
[6] Y. Wang, W. B. Laing, J. von Stecher, and B. D. Esry, Phys. Rev. Lett. **108**, 073201 (2012).
[7] D. Blume and Y. Yan, Phys. Rev. Lett. **113**, 213201 (2014).
[8] K. Helfrich and H.-W. Hammer, J. Phys. B **44**, 215301 (2011).
[9] B. Bazak, J. Kirscher, S. König, M. P. Valderrama, N. Barnea, and U. van Kolck, Phys. Rev. Lett. **122**, 143001 (2019).
[10] L. Contessi, J. Kirscher, and M. P. Valderrama, Phys. Lett. A **408**, 127479 (2021).
[11] O. I. Kartavtsev and A. V. Malykh, J. Phys. B: At. Mol. Opt. Phys. **40**, 1429 (2007).
[12] D. S. Petrov, C. Salomon, and G. V. Shlyapnikov, Phys. Rev. Lett. **93**, 090404 (2004).

[13] P. Naidon and S. Endo, Rep. Prog. Phys. **80**, 056001 (2017).
[14] U. van Kolck, Nucl. Phys. A **645**, 273 (1999).
[15] P. F. Bedaque, H.-W. Hammer, and U. van Kolck, Phys. Rev. Lett. **82**, 463 (1999).
[16] P. F. Bedaque, H.-W. Hammer, and U. van Kolck, Nucl. Phys. A **676**, 357 (2000).
[17] A. Brandstädt, V. B. Le, and J. P. Spinrad, *Graph Classes: A Survey* (Society for Industrial and Applied Mathematics, Washington, D.C., 1999).
[18] Y. Suzuki and K. Varga, *Stochastic Variational Approach to Quantum-Mechanical Few-Body Problems*, Lecture Notes in Physics Monographs (Springer, Berlin, 1998).
[19] H. Hofmann, in *Proceedings of the Eighth Autumn School on the Models and Methods in Few-Body Physics, Lisboa, Portugal, October 13–18, 1986*, 1st ed., edited by L. S. Ferreira, A. C. Fonseca, and L. Streit, Lecture Notes in Physics (Springer, Berlin, Heidelberg, 1987), p. 243.
[20] S. König, H. W. Grießhammer, H.-W. Hammer, and U. van Kolck, Phys. Rev. Lett. **118**, 202501 (2017).
[21] J. von Stecher, J. Phys. B **43**, 101002 (2010).
[22] B. Bazak, M. Eliyahu, and U. van Kolck, Phys. Rev. A **94**, 052502 (2016).
[23] N. J. A. Sloane and T. O. F. Inc. (2020), http://oeis.org/?language=english.
[24] M. L. Stein and P. R. Stein (1963), https://www.osti.gov/biblio/4180737.
[25] D. V. Fedorov and A. S. Jensen, Phys. Rev. Lett. **71**, 4103 (1993).
[26] H.-W. Hammer and L. Platter, Eur. Phys. J. A **32**, 113 (2007).
[27] J. von Stecher, J. P. D'Incao, and C. H. Greene, Nat. Phys. **5**, 417 (2009).
[28] A. Deltuva, Phys. Rev. A **82**, 040701(R) (2010).
[29] S. K. Adhikari, T. Frederico, and I. D. Goldman, Phys. Rev. Lett. **74**, 487 (1995).
[30] M. R. Hadizadeh, M. T. Yamashita, L. Tomio, A. Delfino, and T. Frederico, Phys. Rev. Lett. **107**, 135304 (2011).
[31] T. Frederico, W. de Paula, A. Delfino, M. T. Yamashita, and L. Tomio, Few-Body Syst. **60**, 46 (2019).
[32] P. Naidon, Few-Body Syst. **59**, 64 (2018).